Proceedings of the 1999 IEEE/RSJ
International Conference on
Intelligent Robots and Systems

Tele-Touch Feedback of Surfaces at the Micro/Nano Scale: Modeling and Experiments

Metin Sitti, Satoshi Horiguchi, and Hideki Hashimoto
Institute of Industrial Science, University of Tokyo
Roppongi, 7-22-1, Minato-ku, Tokyo, 106-8558, Japan
{sitti,hideki}@vss.iis.u-tokyo.ac.jp

Abstract

In this paper, a teleoperated micro/nano scale touching system is proposed, and micro/nano contact mechanics models are introduced. Using a 1-DOF haptic device, force-reflecting servo type scaled teleoperation controller, and Atomic Force Microscopy cantilever tip, touching experiments and Virtual Reality Simulator for micro/nano-touch are realized. Scaling issue of the micro/nano forces and positions is discussed and possible solutions are proposed. For the first time upon our knowledge, such issue is discussed with nano scale experimental results. Experimental results show that micro/nano contact force feedback can be held for flat surfaces with the proposed system.

1 Introduction

In our daily lives, direct physical interaction/contact with objects such as shaking hands, grasping a glass of water, opening the tap of the bottle, and etc. constitutes one of the most important sensings. However, this kind of direct interactions are limited to only macro scale objects where special tools are needed for interacting with small (micro/nano) scales. Tele-Nanorobotics technology enables such tools, and this study is focused on one of the applications of our Tele-Nanorobotics System [1]: teleoperated physical contact interactions with surfaces at the micro/nano scale. Most of the micro/nano robotics researches does not include the detailed effect of object deformation and adhesion effect during *contact* type of manipulation, and this study also introduces deformation/indentation models for understanding the micro/nano scale contact behaviour in detail.

The main phenomenon at the micro/nano scale is the scaling effect where the gravitational forces become negligible with respect to attractive or repulsive interatomic forces, and object properties change, i.e. objects become more fragile and deformable. Thus, a different mechanics which can be called as *micro/nano mechanics* field is introduced by many researchers [2]. One of the main components of this new field is micro/nano contact mechanics [3]. Surface Force Apparatus and recently Atomic Force Microscopy (AFM) are utilized [4] for understanding the contact phenomenon of surface atoms at the micro/nano scale. AFM can enable single asperity contact studies where local contact studies with very high resolution has become possible. For AFM-based contact/indentation studies, Hertz [5], [6], [7], [8], JKR [9], DMT, BNC and Maugis-Dugdale (MD) [2], [10] models have been proposed. Hertz model is realistic in the case of large external loads with compared to surface adhesion. However, load amounts may not be large during micro/nano manipulation tasks, thus this model should not be utilized in the case of small loads. DMT model can apply well to the rigid surfaces with low adhesion, but may underestimate the true contact area. On the other hand, JKR model adds the effect of adhesion to the Hertz model, and it can be used in the case of small loads. But, it assumes that short-ranged surface forces act only *inside* the contact area, and this may underestimate loading due to the surface forces. Finally, MD model is the recent best model since it is analytical, and does not underestimate surface forces and contact area.

In this paper, micro/nano contact mechanics is connected with tele-robotics approach for putting human operators inside the micro/nano world for touching and physically interacting. This kind of study is important especially for reliable tele-manipulation of micro/nano deformable surfaces such as biological objects. Upon our knowledge, this paper is the first one at this kind of study using micro/nano contact mechanics and teleoperation system. Falvo et al. [11] utilized tele-robotics technology for tele-manipulation,

0-7803-5184-3/99/$10.00 © 1999 IEEE

but did not consider the contact mechanics modeling issue.

Our approach is to utilize Hertz, DMT, JKR, and MD deformation models for a Virtual Reality Micro/Nano Touching Simulator using the AFM, and then results are compared with teleoperated AFM tip touching experiments. For the bilateral teleoperation force feedback control, force-reflecting servo-type controller is used. The scaling problem for this kind of application is defined, and possible solutions are proposed.

2 Problem Definition

AFM cantilever with its sharp tip is replaced by our finger at the micro/nano scale as can be seen in Figure 1. For a contact load P perpendicular to the surface, the position of the surface (or the cantilever base) is controlled through a scaled bilateral teleoperation controller. Other parameters in the figure are as follows: F_m and F_s are the master and slave forces, x_m and x_s are the master and slave positions, and τ_m and τ_s are master and slave control reference inputs. Here, the main issues are the modeling of the micro/nano contact forces where it is different from the macro world contact interaction, designing a scaled bilateral teleopration controller for reliable contact force feedback, and user friendly visual feedback for more intuitive teleoperation control.

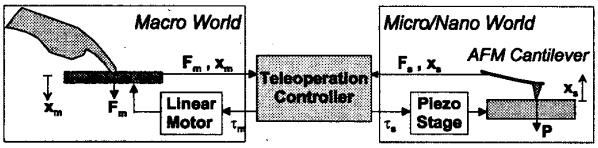

Figure 1: Tele-touch system structure where the human finger is replaced by the AFM cantilever tip at the micro/nano scale.

3 Micro/Nano Contact Mechanics

The contact interaction with the AFM cantilever tip and surface is shown in Figure 2 [5]. Here, the sample is assumed to be an elastically deformable flat half-space, and the mass of the cantilever is assumed to be concentrated on the tip apex. P represents the applied load, α is the cantilever tilt angle for enabling an easier point contact, and k_c, b_c, m_c^*, ζ are the cantilever stiffness, damping constant, effective mass, and deflection respectively. $k_i(z,\zeta)$ and b_i are the *tip-surface interaction stiffness* and *damping*, and δ is the penetration depth. The dynamics of the cantilever can be given as [2]:

$$m_c^*\ddot{\zeta}(t) + 2m_c^* b_c(\dot{\zeta}(t) + k_c\zeta(t) = k_i(z,\zeta)(z(t) - \zeta(t)) + 2m_c^* b_i(\dot{z}(t) - \dot{\zeta}(t) \quad (1)$$

Assuming the damping terms are negligible, and removing the time $t \in R$ for the notation simplicity:

$$m_c^*\ddot{\zeta} + k_c\zeta = k_i(z,\zeta)(z - \zeta) \ . \quad (2)$$

Here, the special cases are: (1) if $k_i >> k_c$, $\zeta = z$ at the equilibrium which means there is no surface deformation, (2) when $k_i = -k_c$, then $m_c^*\ddot{\zeta} = k_i z$. During the contact, applying a load P by moving the cantilever base position z results in the following equalities:

$$\begin{aligned} P(t) &= k_c\zeta(t) \\ \delta(t) &= \Delta(t) - \zeta(t)cos\alpha \\ \Delta(t) &= z(t) - z_0 \ , \end{aligned} \quad (3)$$

where z_0 is the piezo position when the tip contacts to the sample.

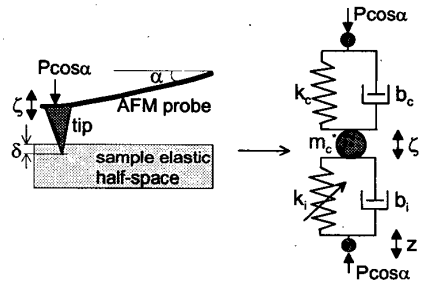

Figure 2: Model for contact-type physical interaction at the micro/nano scale using AFM tip and deformable flat samples.

3.1 Hertz Model

For the Hertz deformation model, load P results in a contact radius a with the general relation of:

$$\begin{aligned} P &= Ka\delta \\ \frac{1}{K} &= \frac{m}{2}\left(\frac{1-\nu_t^2}{E_t} + \frac{1-\nu_s^2}{E_s}\right) \ , \end{aligned} \quad (4)$$

where K is the *reduced elastic modulus* for the tip-sample system, m is the tip geometry dependent constant ($m = 1$ for the cylindirical, $m = 1.5$ for the

spherical, and $m = 2$ for the conical tip case), E_t and E_s are the Young modulus, and ν_t and ν_s are the sample Poison's coefficients respectively. For our system, the AFM tip is spherical with radius $R_c \approx 20-30\ nm$, and using the Hertz model for a sphere-flat object interaction, $a = \sqrt{R_c\delta}$. Then following relation can be computed:

$$\Delta = \delta + \sqrt{R_c}Kcos\alpha\delta^{3/2}/k_c \ . \tag{5}$$

If the tip is very sharp, i.e. $R_c < 10\ nm$, the geometry can be assumed to be conical with the tip half angle ψ where $a = \pi tan\psi\delta/2$. Then,

$$\Delta = \delta + \frac{\pi tan\psi}{2Kk_c}\delta^2 \ . \tag{6}$$

Furthermore, some researchers [7] approximates the contact radius using simple geometry as $a = \sqrt{2\Delta R_c}$ for the spherical tip case, then:

$$\delta = \frac{k_c\Delta}{k_c + Kcos\alpha\sqrt{2\Delta R_c}} \ . \tag{7}$$

3.2 DMT Model

This model accounts for long-ranged attraction around the periphery of the contact area while the defromation geometry is Hertzian such that for a sperical tip and flat surface:

$$\begin{aligned} P &= Ka^3/R_c - 2\pi R_c\omega \\ \delta &= a^2/R_c \ , \end{aligned} \tag{8}$$

where ω is the adhesion energy.

3.3 JKR Model

Adding the short-ranged adhesion forces, for spherical tip and flat surface, JKR model results in following equations:

$$\begin{aligned} P &= Ka^3/R_c - \sqrt{3\pi\omega Ka^3} \\ \delta &= a^2/R_c - 2/3\sqrt{3\pi\omega a/K} \\ a^3 &= (P + 3\pi R_c\omega + \sqrt{6\pi R_c\omega P + (3\pi R_c\omega)^2})R_c/K \end{aligned} \tag{9}$$

3.4 MD Model

By analogy with the plastic zone ahead of a crack, MD model can be used for all cases [1], [2] such that:

$$\begin{aligned} &\frac{\lambda a^2}{2}\frac{K}{\pi R_c^2\omega}^{2/3}[\sqrt{m^2-1} + (m^2-2)cos^{-1}\frac{1}{m} + \\ &\frac{4\lambda^2 a}{3}\frac{K}{\pi R_c^2\omega}^{1/3}[\sqrt{m^2-1}cos^{-1}\frac{1}{m} - m + 1] = 1, \end{aligned}$$

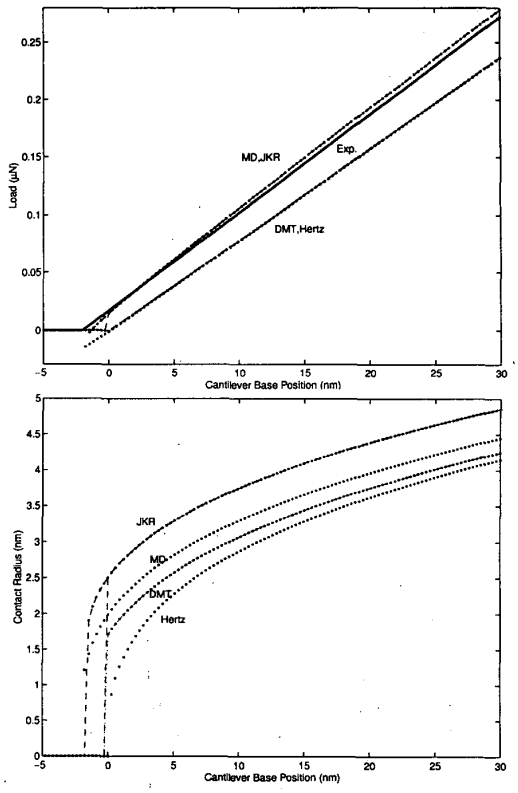

Figure 3: Applied load and contact radius results for Hertz, DMT, JKR and MD models during unloading in the case of silicon tip and substrate (Exp. (solid) in the load graph represents the experimental data).

$$\begin{aligned} \delta &= \frac{a^2}{R_c} - \frac{4\lambda a}{3}\frac{\pi\omega}{R_cK}^{1/3}\sqrt{m^2-1}, \\ P &= \frac{Ka^3}{R_c} - \lambda a^2\frac{\pi\omega K^2}{R_c}^{1/3}[\sqrt{m^2-1} + m^2cos^{-1}\frac{1}{m}] \\ \lambda &= \frac{2.06}{a_0}\left(\frac{R_c\omega^2}{\pi K^2}\right)^{1/3} \end{aligned} \tag{10}$$

where a_0 is the interatomic distance, and m is the ratio of the width of the annular region to a.

For comparing above deformation models, a silicon tip and silicon sample are contacted ($E_{si} = 110\ GPa$, $\nu_{Si} = 0.35$). Assuming a water layer between the tip and sample, $\omega \approx 2\gamma$ where $\gamma = 72mJ/m^2$, indentation force and a vs. Δ curves are held as shown in Figure 3 during unloading/retraction. In the figure, also the real data which is held from the experimental automatic approach and retraction data as the contact unloading slope of $\approx 8.5\ N/m$ is shown. However, the contact radius cannot be directly measured, and the real one is not shown. The results show

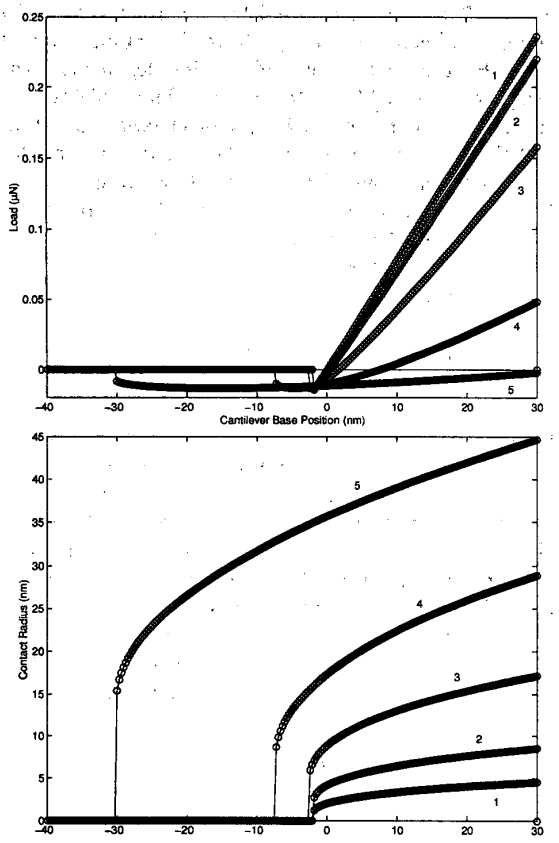

Figure 4: Load (upper) and contact radius (lower) vs. tip base displacement curves for different materials during unloading (E_s=(5) 0.01, (4) 0.1, (3) 1, (2) 10, (1) 100 GPa) using the MD model.

that JKR overestimates the contact area while DMT and Hertz underestimates, and DMT and Hertz models also underestimates the applied load. For different samples with different E_s, MD gives the load and cantact radius data as can be seen in Figure 4. As the surface becomes soft, i.e. E_s is smaller, the contact area is increased while the applied load is decreased. This may cause problems in the force feedback scaling since the same scaling factor may not give the enough scaled feedback on the operator finger for different range of surfaces. One solution is the preliminary calibration of the force scaling factor for all surfaces for optimal force feedback.

4 Bilateral Teleoperation Control

For feeling the scaled nano forces on the human finger, the bilateral teleoperation control system shown in Figure 5 is constructed. A 1 DOF haptic device expained in [1] is used as the master device.

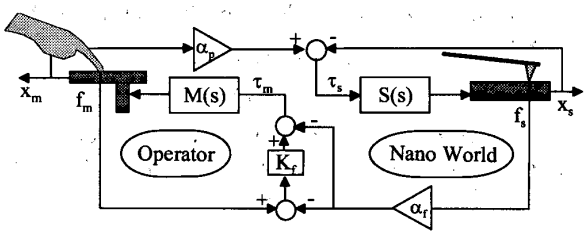

Figure 5: Scaled bilateral teleoperation control system.

4.1 Dynamics Modeling

Force feedback is sensed through the linear motor torque with the master arm dynamics of:

$$m_m\ddot{x}_m + b_m\dot{x}_m = \tau_m + f_m \ , \qquad (11)$$

with m_m is the arm mass, b_m is the damping ratio, f_m and x_m denote the operator force and arm position, and τ_m is the motor driving torque.

For the slave site, AFM tip base position (or sample position) $x_s(t)$ is controlled using Physick Instrumente Co. (P-762.3L) piezoelectric stage with LVDT (Low-Voltage Differential Transformer) integrated sensor is utilized. Closed-loop resolution is limited to 10 nm due to the sensor resolution while in open-loop 1 nm resolution is possbile. The dynamics of the z-axes stage can be given as [12]:

$$\frac{1}{\omega_n^2}\ddot{x}_s + \frac{1}{\omega_n Q}\dot{x}_s + x_s = \tau_s - f_s \ , \qquad (12)$$

where $\omega_n = 2\pi f_n$, $f_n = \sqrt{k_s/m_s}/(2\pi) = 450\ Hz$ is the resonant frequency with m_s and k_s are the stage and sample total mass and k_s is the stage stiffness, $Q = 20$ is the amplification factor, x_s denotes the AFM cantilever base position, f_s is the force that the tip applies to the sample, and τ_s is the stage driving force.

The tip-sample interaction dynamics which is given in Eq. 2 can be written as:

$$f_s = k_c\zeta = -m_c^*\ddot{\zeta} + k_i x_s - k_i\zeta \ , \qquad (13)$$

with $x_s = z$. Assuming quasi-static, i.e. slow, motion which means equilibrium at each x_s displacement:

$$f_s = \frac{k_i(x_s,\delta)k_c}{k_i(x_s,\delta) + k_c}x_s \ . \qquad (14)$$

4.2 Control Scheme

The ideal response of the controller is given as follows:

$$\begin{aligned} x_s &\rightarrow \alpha_p x_m \ , \\ f_m &\rightarrow \alpha_f f_s \ , \end{aligned} \tag{15}$$

at the steady state. Here α_f and α_p are the force and position scaling factors respectively. As the controller, a force-reflecting servo type controller is selected where:

$$\begin{aligned} \tau_m &= -\alpha_f f_s - K_f(\alpha_f f_s - f_m) \\ \tau_s &= K_v(\alpha_p \dot{x}_m - \dot{x}_s) + K_p(\alpha_p x_m - x_s) \ , \end{aligned} \tag{16}$$

K_p and K_v are position control parameters, and K_f is the force error gain. Using the slave and master dynamics equations, and assuming a very hard sample such that $k_i >> k_c$, and $f_s = k_c x_s$, equalities for the ideal response at the steady state are given as follows:

$$\begin{aligned} x_s &= \alpha_p K_p/(1+K_p) x_m \\ f_m &= \frac{1+K_p}{k_c \alpha_p K_f K_p} + \alpha_f(1+1/K_f) \ . \end{aligned} \tag{17}$$

Thus, for enabling the ideal responses, K_p, K_f and α_p should be selected as large as possible.

4.3 Selection of the Scaling Factors

In this paper, the forces and positions are linearly scaled with parameters α_f and α_p. For determining these parameters, there are different approaches. Recently, Goldfarb [13] concluded two cases: (1) $\alpha_f = \alpha_p = L$ for structurally dominated ineteractions, (2) $\alpha_f = \alpha_p^2 = L^2$ for surface-dominated interactions where $L = (x_s^{max} - x_s^{min})/(x_m^{max} - x_m^{min})$, and assuming $L >> 1$. Furthermore, we add also a heuristic one where we can use the maximum range and resolution, i.e. performance, of the master and slave motions and forces. In this case:

$$\begin{aligned} \alpha_p &= (x_s^{max} - x_s^{min})/(x_m^{max} - x_m^{min}) \\ \alpha_f &= (f_m^{max} - f_m^{min})/(f_s^{max} - f_s^{min}) \ , \end{aligned} \tag{18}$$

Upper max and min terms denote the minimum and maximum values for the given parameter. This kind of scaling can be especially useful for micro/nano manipulation cases where the resolution of the stages are limited for long ranges of 10s of micrometers, and environmental disturbances largely reduce the measurement and positioning accuracy.

At first, the measurement limitations should be considered. For the positioning limits, resolution $\delta_p = 10\ nm$ in the closed-loop control case. For the initial height of the tip above the sample contact point H, and a maximum indentation depth δ_{max}, the range $x_s^{max} - x_s^{min} = H + \delta_{max}$. The deflection of the cantilever is limited by the electronics such that $-10S \leq \zeta \leq 10S$ where S is the conversion term for the deflection from $Volt$ to μm. It is calibrated before the experiments (in our case $S = 0.033\ \mu m/Volt$) Thus, $\delta_{max} \leq 10S = 0.33 \mu m$.

For the micro/nano force measurements, the noise in the cantilever deflection measurement system e_c is peak-to-peak 50 mV which means an approximate force resolution $\delta_f = 0.05 k_c S = 13\ nN$. Since ζ is limited, also $-10 k_c S \leq f_s \leq 10 k_c S$. For $k_c = 8\ N/m$, $-2.6\ \mu N \leq f_s \leq 2.6\ \mu N$. However, the attactive micro/nano forces are relatively very small with respect to contact forces, and typically $-0.6\ \mu N \leq f_s \leq 2.6\ \mu N$. Furthermore, due to δ_p, minimum ζ steps are limited to $k_c \delta_p = 80\ nN$. Thus, the overall force resolution in the closed-loop control case is $\delta_f = 90\ nN$. On the other hand, for the open-loop control, there is no limitation from δ_p, and $\delta_f = 13\ nN$.

The resolutions and ranges can be combined for determining the possible number of control steps N_f and N_p for the nano force and position as follows:

$$\begin{aligned} N_p &= (H + \delta_{max})/\delta_p \\ N_f &\leq 20 k_c S/\delta_f \ . \end{aligned} \tag{19}$$

For the case of $\delta_{max} = 0.3 \mu m$ and $H = 0.1 \mu m$, $N_p = 40$ and $N_p = 400$, and using above values $N_f = 58$ and $N_f = 400$ for the $\delta_p = 10\ nm$ and $\delta_p = 1\ nm$ cases. For an accurate control, N_p and N_f should be as large as possible. Therefore, 10 nm resolution may not be enough for precise feedback, and 1 nm resolution should be utilized.

For the master device, the motion range is limited to 2 cm with $\delta_p = 0.004\ cm$. Thus, $N_p = 500$ for the master positioning which is enough. Force measurement resolution is $\delta_f = 0.02\ N$ for the strain gauge sensors including the electronics noise, and the maximum measurable range is approximately $\pm 5\ N$. Thus, $N_f \leq 500$ which is enough. Finally,

$$\begin{aligned} \alpha_p &= (H + \delta_{max})/2.0\ (\mu m/cm) \\ \alpha_f &= (f_m^{max} - f_m^{min})/3.2\ (N/\mu N) \ . \end{aligned} \tag{20}$$

For applying the scaling rules (1) and (2), H or f_m^{max} can be arranged for enabling the scaling rule equalities.

5 Virtual Reality Visulator and Simulator for Tele-Touch

The intutive visual display is held by AFM scanning of the surface, and displaying the 3-D graphics of the surface and the AFM tip helps to the operator as shown in Figure 6 [14]. For simulating the micro/nano touch, a Virtual Reality (VR) Simulator is constructed for freely changing the parameters, and initial training. A sample interface graphics can be seen in Figure 7. Moreover, a realistic simulator will enable a real-time animator display for real-time nano manipulation monitoring. Using the haptic device, and the micro/nano contact mechanics models, touching experiments are realized.

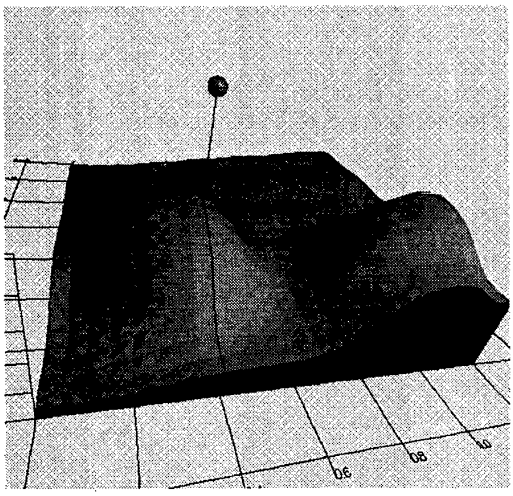

Figure 6: Virtual Reality Visulator during touching experiments: interactive AFM scanned substrate shaded image, and real-time AFM tip position (as a spherical ball) displays.

6 Experiments

During the experiments, a piezoresistive cantilever (Park Scientific Inst.^{TM}) with silicon tip and parameters of $R_c = 20\ nm$, $k_c = 8\ N/m$ and $S = 0.033\ \mu m/Volt$ is utilized [1]. VR Nano Visulator graphics display [15] is used for observing the real-time tip position during touching. Touching to a silicon sample with 40% humidity conditions, resulting master and scaled slave position and forces can be seen in Figure 8. Experimental parameters are $K_f = 2$, initial tip height $H = 0.6\ \mu m$, $\alpha_p = 4 \times 10^3$ and $\alpha_f = 2 \times 10^6$. In the force figure, the bottom of the zero line represents the attractive forces, and the above the zero line is the repulsive forces. Thus, the point B corresponds to the approach attractive force peak due to the non-contact forces, the point C do the repulsive/contact force peak, and finally A do the retraction atractive force peak due to the adhesion forces. Results show that ideal responses for the positions and forces are held successfully. But, in the force curves, the approach attractive slave forces are almost not able to be tracked since this part is highly nonlinear, and the liquid layer on the surface causes the tip to jump fastly to the contact wit the surface. Moreover, the positioning accuracy during the experiment is around 10 nm which is not enough fror stable imaging of the approach attractive peak. Therefore, the resolution of the stage will be decreased in the near future down to the subnanometers with integrated capacitive sensors instead of LVDT sensors.

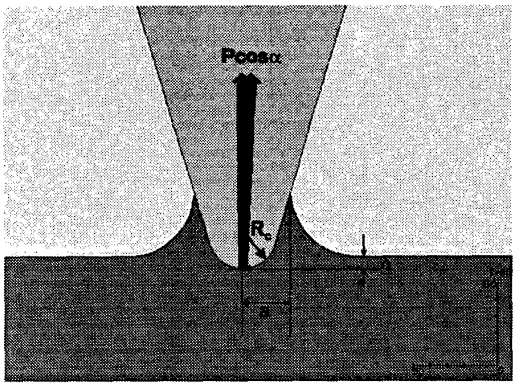

Figure 7: Virtual Reality Simulator for AFM tip-substrate 1-DOF contact interaction.

7 Conclusion

In this paper, a teleoperated micro/nano scale touching system is proposed, and micro/nano contact mechanics models are introduced. Using a 1-DOF haptic device, and force-reflecting servo type scaled teleoperation controller, touching experiments and VR Simulator-based simulations are realized. Scaling issue of the micro/nano force and position is discussed and possible solutions are proposed. Experimental and simulation results show that approach non-contact attractive forces are difficult to feel with the present system, but in the other parts and the present system can supply the surface compliance feedback with obeying to the ideal kinesthetic response. This kind of application can enable reliable

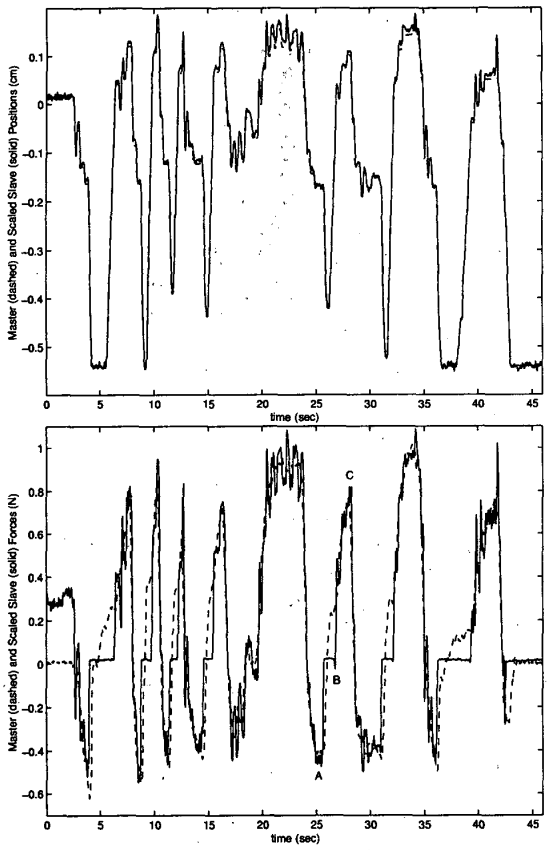

Figure 8: Touching results to a silicon sample with silicon tip: master (dashed) and scaled slave (solid) positions (upper) and forces (lower) data.

manipulation of micro/nano deformable objects such as biological ones. Future works are the adding micro/nano friction models to the contact mechanics for enabling 3-DOF VR Tele-Touch Simulator, and adding micro/nano objects into the VR environment for micro/nano manipulation simulations which can be used for micro/nano object assembly and manipulation task-planning, training and real-time monitoring interface.

References

[1] M. Sitti and H. Hashimoto, "Tele-nanorobotics using atomic force microscope," in *Proc. of the IEEE/RSJ Int. Conf. on Intelligent Robots and Systems*, pp. 1739–1746, Canada, Oct. 1998.

[2] N. A. Burnham and A. J. Kulik, "Surface forces and adhesion," *Handbook of Micro/Nanotribology*, pp. 247–271, Dec. 1997.

[3] K. Johnson, "A continuum mechanics model of adhesion and friction in a single asperity contact," *Micro/Nanotribology and its Applications, Kluwer Ac. Pub.*, pp. 151–168, 1997.

[4] B. Brushan, *Micro/Nanotribology and Its Applications*. Kluwer Academic, Vol. E330, 1997.

[5] M. R. VanLandingham, S. H. McKnight, and et al., "Relating elastic modulus to indentation response using atomic force microscopy," *J. of Materials Science Letters*, 1996.

[6] M. Sitti and H. Hashimoto, "Two-dimensional fine particle positioning using a piezoresistive cantilever as a micro/nano-manipulator," in *Proc. of the IEEE Int. Conf. on Robotics and Automation*, pp. 2729–2735, Detroit, May 1999.

[7] J. Tamayo and R. Garcia, "Deformation, contact time, and phase contrast in tapping mode scanning force microscopy," *Langmuir*, vol. 12, no. 18, pp. 4430–4435, 1996.

[8] R. W. Stark, S. Thalhammer, and et al., "The afm as a tool for chromosomal dissection - the influence of physical parameters," *Appl. Phys. A*, vol. 66, pp. 579–584, 1998.

[9] D. Sarid, J. P. Hunt, R. K. Workman, and et al., "The role of adhesion in tapping-mode atomic force microscopy," *Appl. Phys. A*, no. 66, pp. 283–286, 1998.

[10] N. A. Burnham, O. Behrend, and et al., "How does a tip tap?," *Nanotechnology*, vol. 8, pp. 67–75, 1997.

[11] M. Falvo, R. Superfine, S. Washburn, and et al., "The nanomanipulator: A teleoperator for manipulating materials at the nanometer scale," in *Proc. of the Int. Symp. on the Science and Technology of Atomically Engineered Materials*, pp. 579–586, Nov 1995.

[12] T. R. Hicks and P. D. Atherton, *The Nano Positioning Book*. Queensgate Inst. Ltd., 1997.

[13] M. Goldfarb, "Dimensional analysis and selective distortion in scaled bilateral telemanipulation," in *ICRA*, pp. 1609–1614, 1998.

[14] M. Sitti and H. Hashimoto, "Teleoperated nano scale object manipulation," *Recent Advances on Mechatronics*, pp. 322–335, edited by O. Kaynak, S. Tosunoglu and M.J. Ang, Springer Verlag Pub., Singapore, 1999.

[15] S. Horiguchi, M. Sitti, and H. Hashimoto, "Virtual reality user interface for teleoperated nanometer scale object manipulation," in *Proc. of the IEEE Int. Workshop on Robot and Human Communication*, pp. 142–147, Takamatsu, Japan, Sep. 1998.